Supporting Information

Hierarchically porous $FeNi_3$@FeNi layered double hydroxide nanostructures: One-step fast electrodeposition and highly efficient electrocatalytic performances for overall water splitting

Zihao Liu, Shifeng Li, Fangfang Wang, Mingxia Li and Yonghong Ni*

College of Chemistry and Materials Science, Key Laboratory of Functional Molecular Solids, Ministry of Education, Anhui Provincial Engineering Laboratory for New-Energy Vehicle Battery Energy-Storage Materials, Anhui Normal University, 189 Jiuhua Southern Road, Wuhu, 241002, PR China. Fax: +86-553-3869303. E-mail: niyh@mail.ahnu.edu.cn

Characterization

A Bruker D8 Advanced X-ray diffractometer (XRD, German) was used for analyzing the phase of the as-deposited catalyst. The morphology and EDS mapping images of the catalyst were obtained on a field emission scanning electron microscope (FESEM) equipped with an energy dispersive X-ray analyzer, employing an accelerating voltage of 5/15 kV (15 kV for mapping; Hitachi-8100, Japan). The microstructure was investigated on a transmission electron microscope (TEM, Hitachi-7700, Japan). HRTEM images and SAED were obtained on a JEM-ARM 200F high-resolution transmission electron microscope with the operating voltage of 200 kV. An ESCALAB 250 XPS instrument with a monochromatic Al Kα (hν = 1486.6 eV) was employed for analyzing the chemical state of the as-deposited catalyst. The contact angle experiments were carried out on a surface analyzer (Theta, Attention) at room temperature, employing 4μL of the deionized water droplets. The Raman spectra were recorded using a Raman spectrometer (RENISHAW inVia system, U.K.) with a 532 nm He/Ne laser as the excitation source. UV-vis absorption spectra were recorded on a Metash 6100 UV-vis absorption spectrophotometer (Shanghai).

Electrochemical tests

Electrochemical performance was measured at room temperature on a CHI 660E electrochemical workstation (CHI Instruments, Shanghai, China) with a conventional three-electrode system in 1.0 M KOH **(pH=13.72)**, employing NF loaded by catalysts, Hg/HgO and graphite rod as the working electrode, the reference electrode, and the counter electrode, respectively. **All measured**

potentials were normalized versus the reversible hydrogen electrode (RHE) and the Ohmic resistance is corrected according to the following equations:

$$E_{RHE} = E_{Hg/HgO} + 0.098 + 0.059 \times pH \quad (1)$$

$$E = E_{RHE} - i \times 85\% R_u \quad (2)$$

Where E is the iR-corrected potential, E_{RHE} is the measured potential with respect to RHE (reversible hydrogen electrode), $E_{Hg/HgO}$ and i are experimentally measured potential and current, respectively, and R_u is the uncompensated resistance as determined by electrochemical impedance spectroscopy (EIS) test, which is performed at open-circuit potential and scan from 100 kHz to 0.01 Hz with a voltage perturbation of 5 mV. The impedance at the high frequency limit will approach the uncompensated series resistance as the capacitive impedances trend toward zero.[1-6] Before test, the KOH electrolyte was purged with Ar for 30 min to remove dissolved impurity gas.[7] All electrodes are activated and stabilization by a chronopotentiometry for 10 min at 10 mA cm^{-2} before the CV test, and then the EIS spectra was recorded. The Cyclic voltammograms (CV) curves of HER and OER tests were obtained at a scan rate of 1 mV s^{-1} and the background correction is performed by averaging the positive-going and negative-going scan of CV, resulting in one polarization curve.[1,7,8] The CV curves of overall water splitting was obtained using a H-type electrolyzer equipped with commercial alkaline anion exchange membranes (AEM, Fumatech FAA-3) at a scan rate of 1 mV s^{-1}.[6] The distance between anode and cathode is ~8 cm and the digital photo of AEM electrolyzer is shown in Figure S12. By fitting the linear portion between overpotential (η) and log current (log j) with the equation $\eta = a + b \log(j)$, the corresponding Tafel plots were obtained. Thus, the Tafel slopes (b) of the electrodes were gained. The long-term stability was tested through the chronopotentiometry method at a constant current density without iR compensation. The C_{dl} values for various working electrodes were evaluated from the cyclic voltammogram (CV) in the double-layer region without faradaic processes. The potentials were recorded between 0.923 and 1.023 V at the scanning rate of 20 ~ 100 mV s^{-1} with an interval of 20 mV s^{-1}.

Herein, we have conducted standard experimental calibrations of reference electrode in a three-electrode system with Pt wire as both the working and the counter electrodes in 1.0 M KOH (pH = 13.72). Cyclic voltammograms (CV) were performed at the scan rate of 1 mV/s and the fitting curve was obtained by averaging the forward and backward CV curves.[9] The potential values at zero current were taken to be the thermodynamic potential for the hydrogen evolution reaction. The measured value was 0.903 V, which was very close to the theoretical value of 0.907 V.

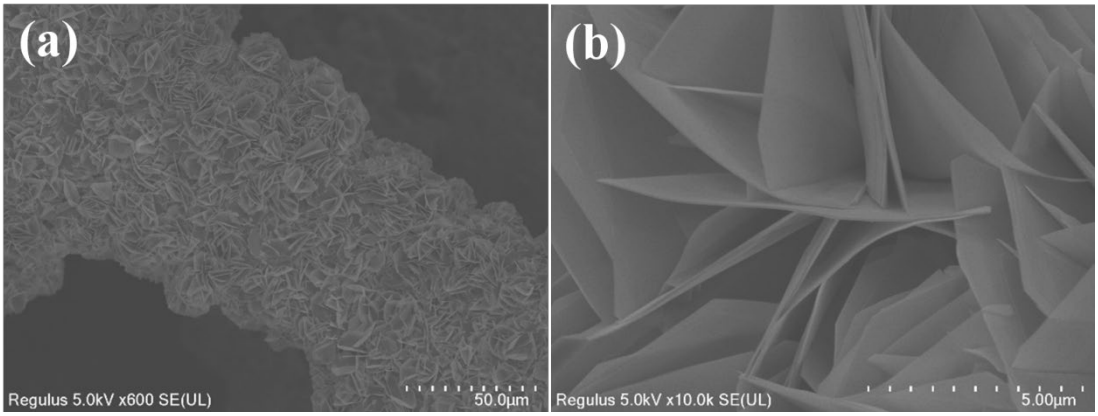

Figure S1. FESEM images of the as-obtained HT-FeNi LDH/NF.

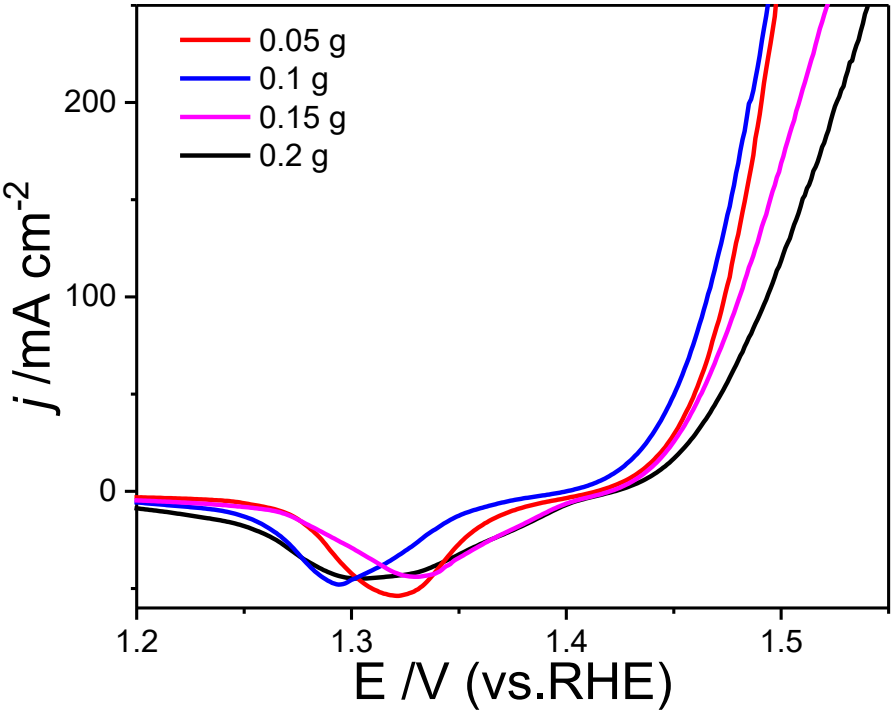

Figure S2. LSV curves **(95% auto iR-corrected and scanned from high potential to low potential)** of $FeNi_3$@FeNi LDH/NF electrodes deposited from the systems with different original amounts of $FeCl_2 \cdot 4H_2O$.

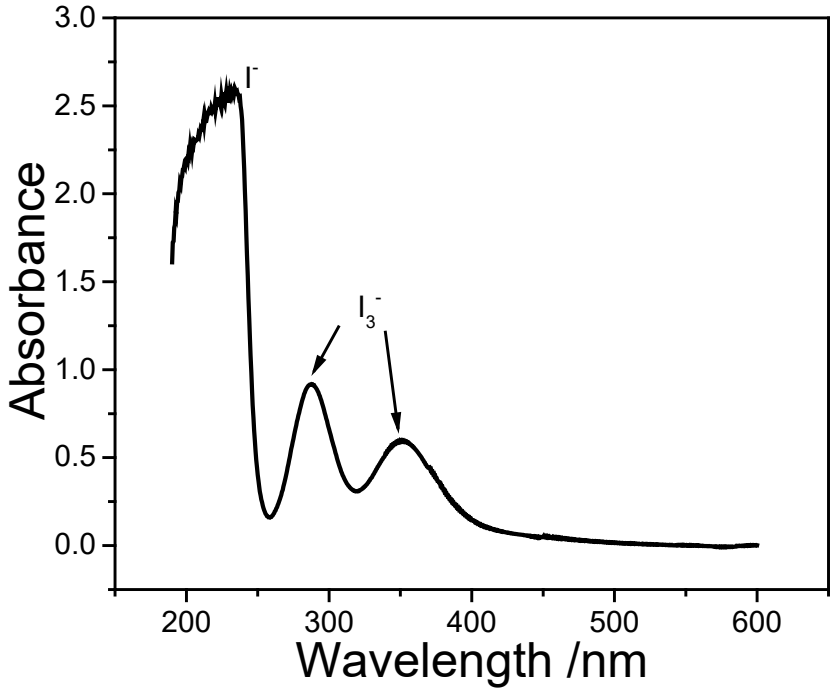

Figure S3. The UV-vis absorption spectrum of the solution near the anode.

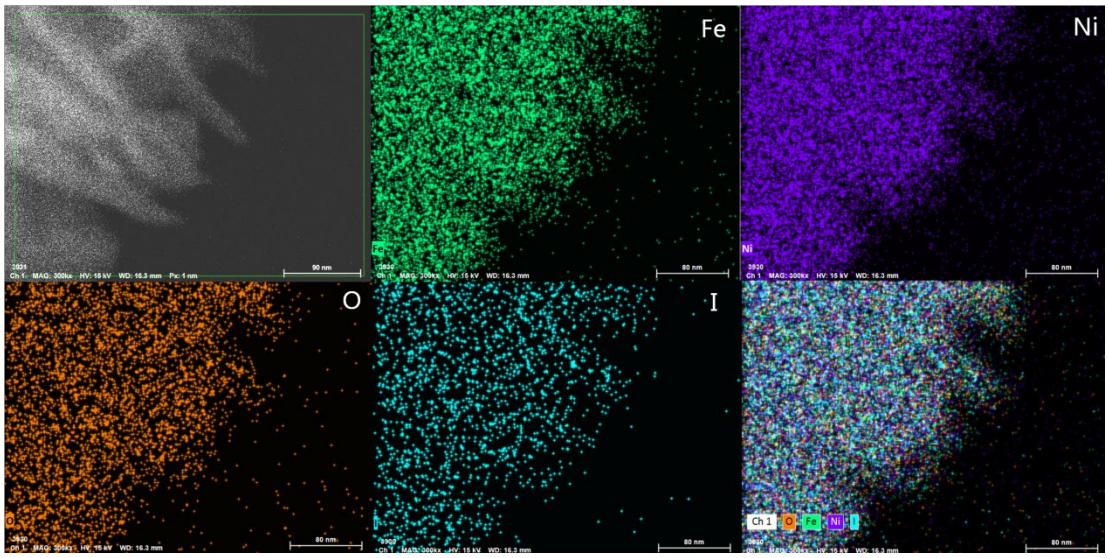

Figure S4. EDS mapping images of various elements in the as-constructed catalyst.

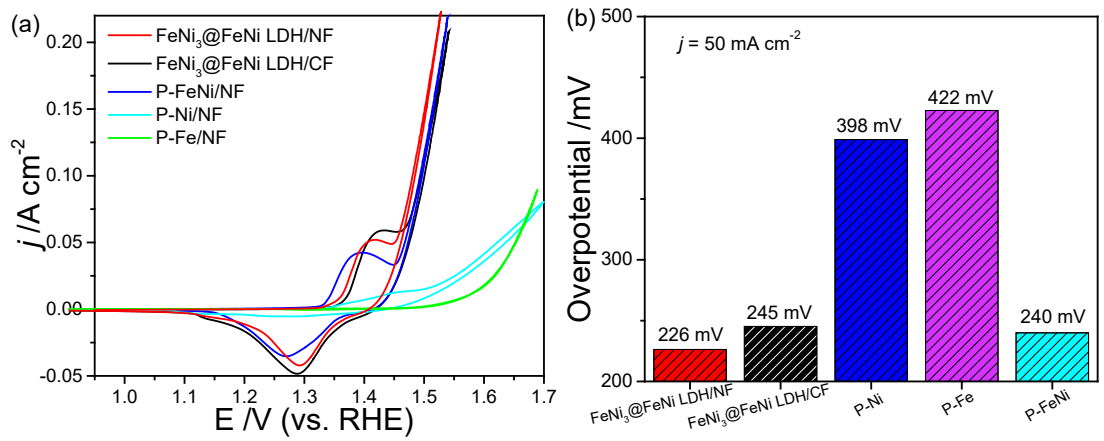

Figure S5. (a) CV curves with 85% manual iR-corrected and (b) Overpotentials at 50 mA cm^{-2} of various electrodes prepared from different electrolytes or substrates. Here, P-FeNi/NF, P-Ni/NF and P-Fe/NF stand for the products prepared from the electrolyte without KI, $FeCl_2$ or $NiCl_2$, respectively; CF represents the Cu foam substrate.

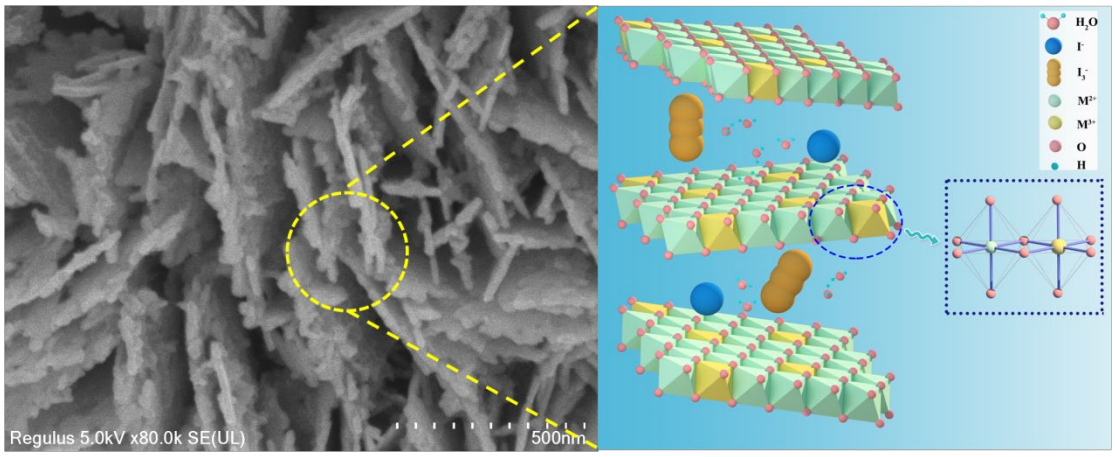

Figure S6. A representative FESEM image of the as-constructed $FeNi_3$@FeNi LDH and the scheme of triiodide anions intercalating FeNi LDH.

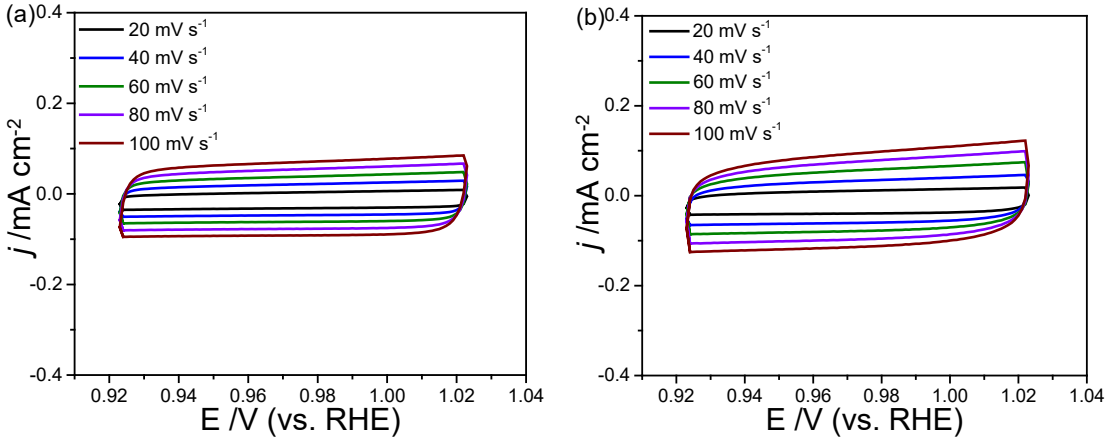

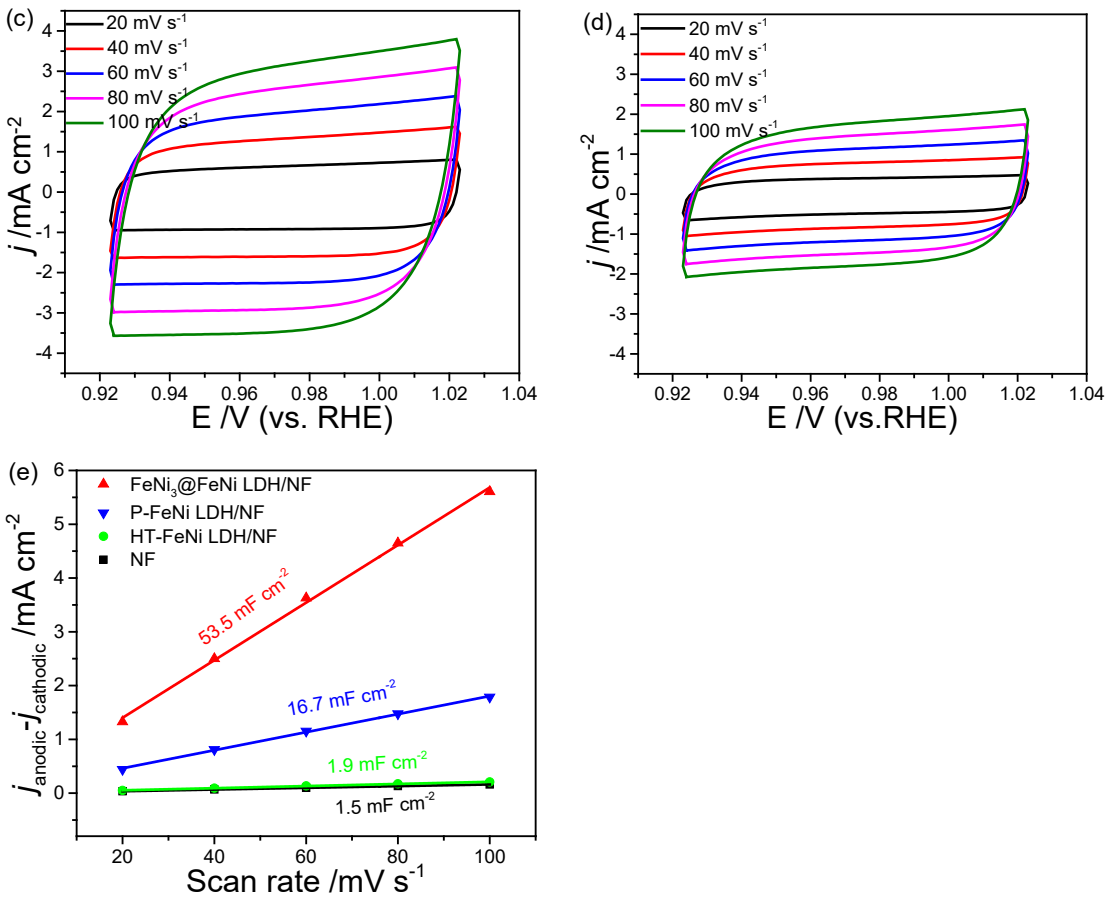

Figure S7. CV curves of various electrodes in the potential window of 0.923-1.023 V at the scan rates of 20, 40, 60, 80, and 100 mV s^{-1}: (a) bare NF, (b) HT-FeNi LDH/NF, (c) $FeNi_3$@FeNi LDH/NF and (d) **P-FeNi/NF. (e) Correlations between the Δj (= j_{anodic} - $j_{cathodic}$) and the scan rates of $FeNi_3$@FeNi LDH, P-FeNi/NF, HT-FeNi LDH and NF, respectively.**

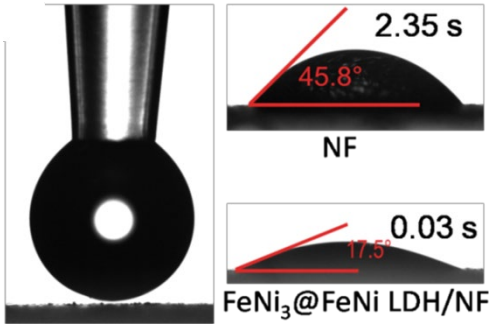

Figure S8. Contact angle measurements of the $FeNi_3$@FeNiLDH/NF and the bare NF.

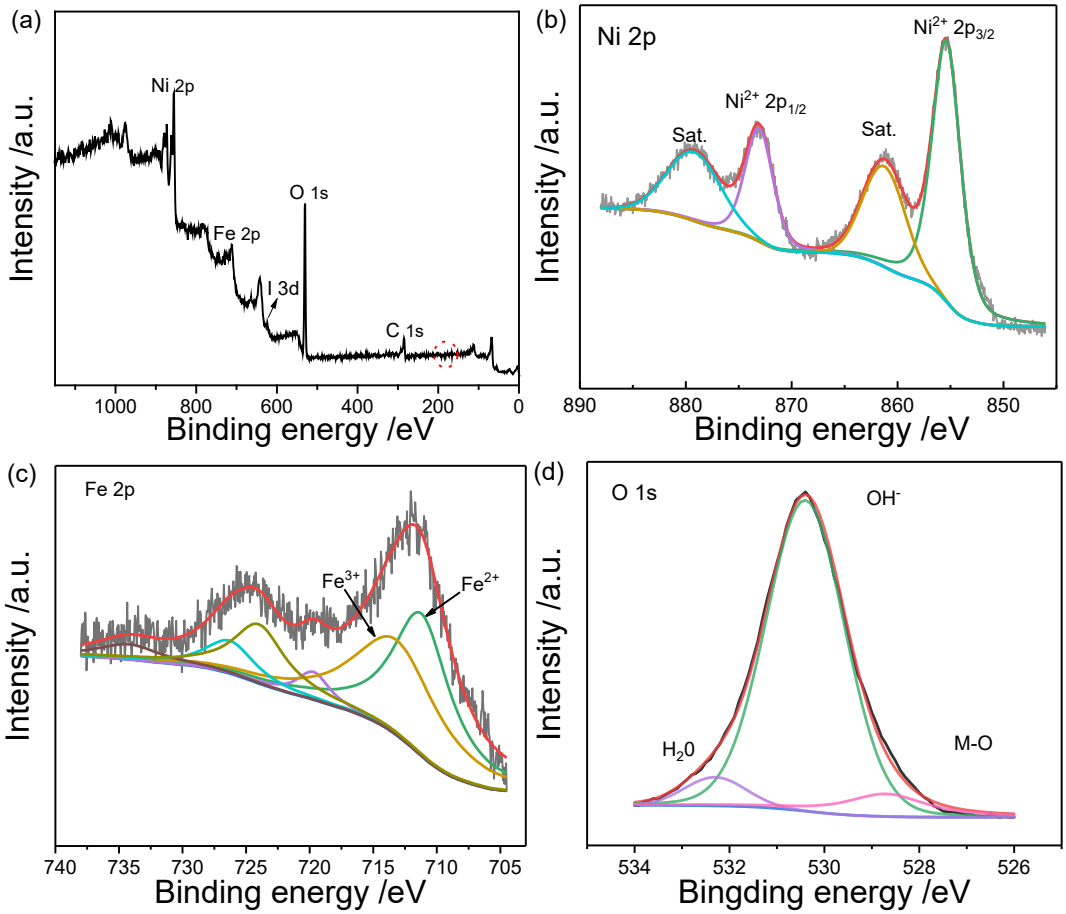

Figure S9. XPS analyses after CV activation: (a) survey spectrum, (b) Ni 2p, (c) Fe 2p and (d) O 1s spectra.

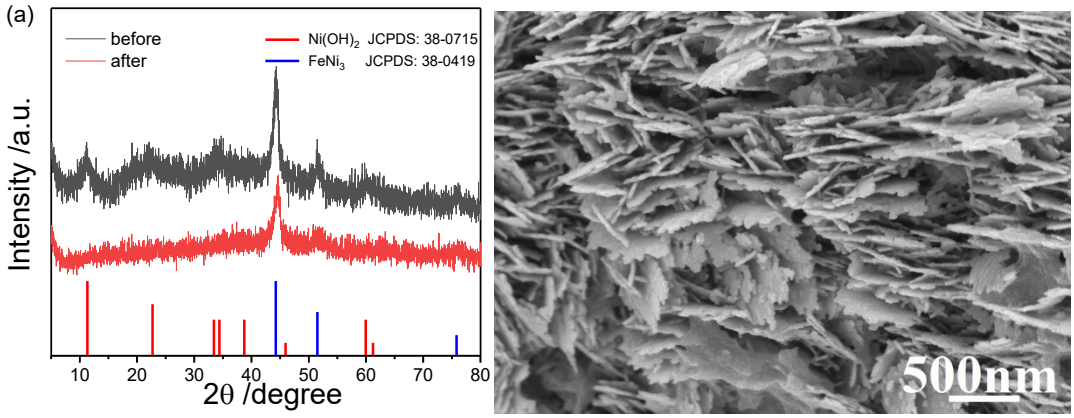

Figure S10. (a) XRD pattern and (b) SEM image of the as-deposited $FeNi_3$@FeNi LDH catalyst after 50 h OER test.

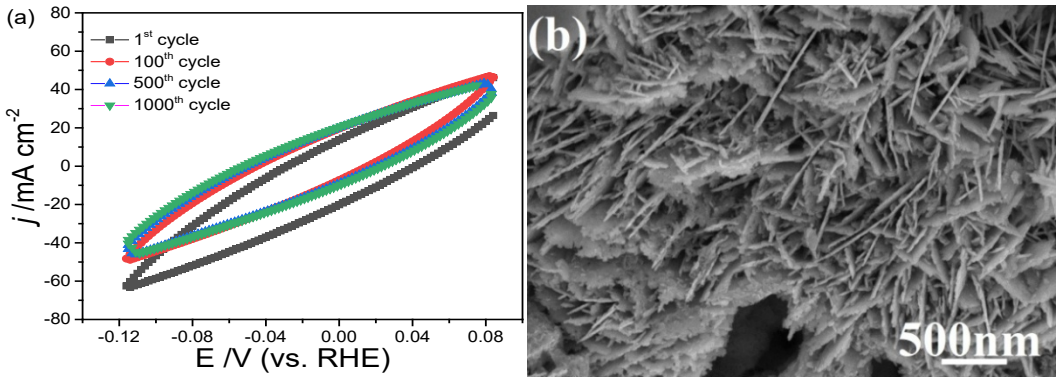

Figure S11. (a) **The CV curves of the 1st, 100th, 500th and 1000th cycles** at 100 mV s^{-1}, and (b) FESEM image of $FeNi_3$@FeNi LDH after HER stability test for 24 h.

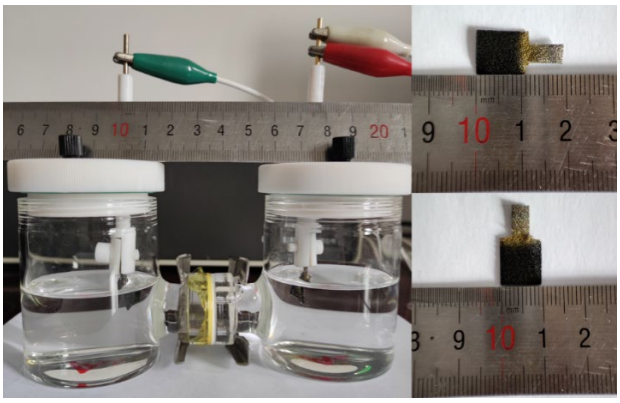

Figure S12. The digital photos of H-type electrolyzer with alkaline anion exchange membranes (Left) and the size of the working electrode (right).

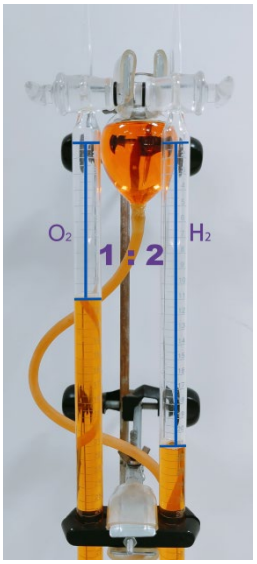

Figure S13. The photograph of the as-used Hoffman apparatus setup.

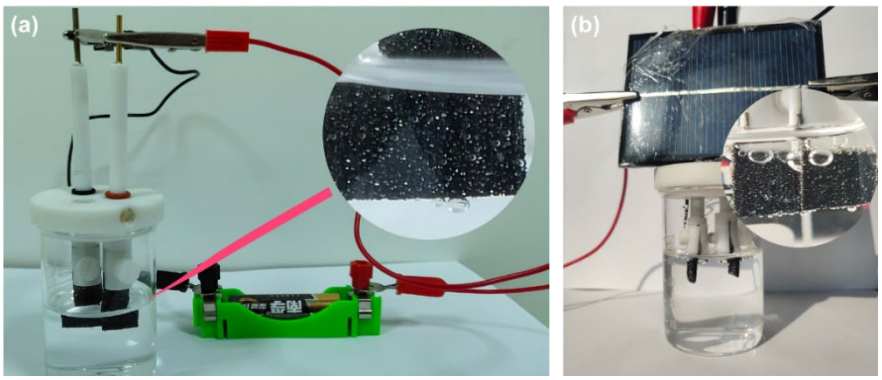

Figure S14. Digital photographs of water electrolysis driven by (a) commercial AA battery of 1.5 V or (b) commercial solar cell.

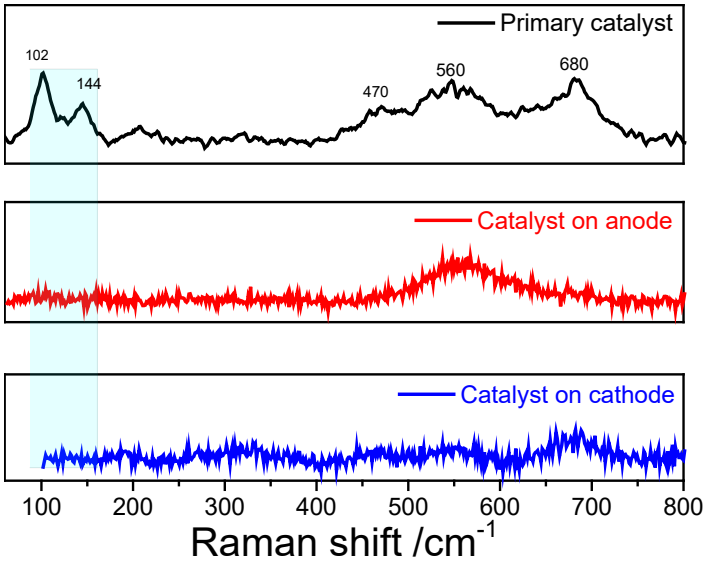

Figure S15. The Raman spectra of **the catalyst after the durability test.**

Table S1. The mass loading densities of various electrodes after electrodeposition.

Electrode	Mass of the electrode (g)		Average Mass loading density (g cm^{-2})
	Before deposition	After deposition	
$FeNi_3$@FeNi LDH/NF	0.2175	0.2520	0.0115
$FeNi_3$@FeNi LDH/CF	0.3355	0.3749	0.0131
P-FeNi /NF	0.2290	0.2657	0.0122
P-Fe /NF	0.2293	0.2304	0.0004
P-Ni /NF	0.2166	0.2604	0.0146

Table S2. Comparison of some representative OER catalysts recently reported for alkaline solution.

Catalyst	η(mV vs. RHE)	Current density (mA cm^{-2})	Tafel slope (mV dec^{-1})	Ref.
$FeNi_3$@FeNiLDH	**199**	**10**	**51.4**	**This work**
N-NiCo LDHs	190	10	46	10
NiFe LDH/NF	215	10	28	11
MoFe:$Ni(OH)_2$/NiOOH	240	10	47	12
NiFe LDH-NS@DG10	210	10	52	13
Ni@NiFe LDH	218	10	66.3	14
NiFe -LDH NSs	280	10	68	15
NiFe-LDH/CNT	247	10	31	16
Cr-doped FeNi-P/NCN	240	10	72.3	17
$FeCo_{0.5}Ni_{0.5}$-LDH	248	10	38	18
$Ni_{0.04}Fe_{0.16}Co_{0.8}Se_2$	230	10	39	19

Table S3. Comparison of some representative HER catalysts recently reported for alkaline solution.

Catalyst	η(mV vs. RHE)	Current density ($mA\ cm^{-2}$)	Tafel slope ($mV\ dec^{-1}$)	Ref.
$FeNi_3$@FeNiLDH	**106**	**10**	**122**	This work
N-NiCo LDHs	100	10	123	10
Ni@NiFe LDH	92	10	72.3	14
CoFe @NiFe-200/NF	240	10	88.8	20
$FeCo_2S_4$@CoFe LDH	115	10	72.8	21
NiFe-NCs	197	10	130	22
Ni_7S_6-F	98	10	77	23
(Ni, Fe)S_2@MoS_2	130	10	101	24
Ni NTAs/NF	101	10	101	25
NiCoFe-PS	97.8	10	51.8	26
Ru/NiFe LDH-F/NF	115.6	10	87.1	27
Ni_5Fe LDH@NF	133	10	89	28

Table S4. Comparison of water splitting performances of the as-prepared $FeNi_3$@FeNi LDH catalyst with some other high-efficiency electrocatalysts reported recently.

Catalyst		$\eta_{10\ mA\ cm^{-2}}$	Tafel slope ($mV\ dec^{-1}$)	OWS Stability		Ref.
				J ($mA\ cm^{-2}$)	Time (h)	
FeNi@FeNi	HER	127	143.1	50	20.3	29
	OER	193	109			
Fe@Ni nanofibers	HER	55	53.5	10	20	30
	OER	230	37.5			
U-Fe-β-$Ni(OH)_2$/NF-2	HER	121	85.19	10	60	31
	OER	218	46.6			
Fe1-NiCoP	HER	60	51.1	10	25	32
	OER	293	37.8			
$Ni_{1-x}Fe_x$-LDH	HER	205	98	1.7 V	24	33
	OER	235	72			
$FeNi_3$-Fe_3O_4 NPs/MOF-CNT	HER	108	96.75	360 mV	20	34
	OER	247	37			
Fe_2P-Co_2P/CF	HER	81	56	100	16.7	35
	OER	185	51			
Ni-Fe-P	HER	66	60	100	10	36
	OER	198	60			
Fe-Ni_3S_2/NF	HER	314(η_{100})	108	10	50	37
	OER	269(η_{100})	85			
Fe-Ni phosphide	HER	116	68	10	80	38
	OER	235	76			
Ni-Fe-$K_{0.23}MnO_2$ CNFs-300	HER	116	103.9	10	24	39
	OER	270	42.3			
NiCoFePS/NF	HER	97.8	51.8	10	200	40
	OER	195	36.7			
Ni/NiFeMoO_x/NF	HER	22	76	500	100	41
	OER	255	35			
$FeNi_3$@FeNi LDH	HER	106	122	10	168	**Thiswork**
	OER	199	51.4			

Reference

1 C. Wei, R. R. Rao, Y.L. Peng, B.T. Huang, I.E.L. Stephens, M. Risch, Z.C. J. Xu, Y. Shao-Horn, *Adv. Mater.* **2019**, *31*, e1806296.

2 M. B. Stevens, L. J. Enman, A. S. Batchellor, M. R. Cosby, A. E. Vise, C. D. M. Trang, S. W. Boettcher, *Chem. Mater.* **2017**, *29*, 120-140.

3 C.C.L. McCrory, S.H. Jung, I. M. Ferrer, S. M. Chatman, J.C. Peter, T.F. Jaramillo, *J. Am. Chem. Soc.* **2015**, *137*, 4347-4357.

4 S.H. Jung, C. C. L. McCrory, I. M. Ferrer, J. C. Peters, T. F. Jaramillo, *J. Mater. Chem. A* **2016**, *4*, 3068-3076.

5 D. Voiry, M. Chhowalla, Y. Gogotsi, N. A. Kotov, Y. Li, R. M. Penner, R. E. Schaak, P. S. Weiss, *ACS nano* **2018**, *12*, 9635-9638.
6 D.Y. Xu, M. B. Stevens, M.R. Cosby, S. Z. Oener, A. M. Smith, L. J. Enman, K. E. Ayers, C. B. Capuano, J. N. Renner, N. Danilovic, Y.G. Li, H.Z. Wang, Q.H. Zhang, S. W. Boettcher, *ACS Catal.* **2019**, *9*, 7-15.
7 W.R. Zheng, M.J. Liu, L. Y. S. Lee, *ACS Energy Lett.* **2020**, *5*, 3260-3264.
8 S.N. Sun, H.Y. Li, Z.C. J. Xu, *Joule* **2018**, *2*, 1024-1027.
9 S.Q. Niu, S.W. Li, Y.C. Du, X.J. Han, P. Xu, *ACS Energy Lett*. **2020**, *5*, 1083-1087.
10 T.L. Chen, R. Zhai, G.L. Chen, J. Huang, W. Chen, X.Q. Wang, D.L. Chen, C.R. Li, K. Ostrikov, *Catal. Today*. **2019**, *337*, 147-154.
11 X. Lu, C. Zhao, Nat. Commun. 2015, 6, 6616.
12 Y. Jin, S. Huang, X. Yue, H. Du, P.K. Shen, ACS Catal. 2018, 8, 2359-2363.
13 Y. Jia, L. Zhang, G. Gao, H. Chen, B. Wang, J. Zhou, M.T. Soo, M. Hong, X. Yan, G. Qian, J. Zou, A. Du, X. Yao, Adv. Mater. 2017, 29, 1700017.
14 Z. Cai, X. Bu, P. Wang, W. Su, R. Wei, J.C. Ho, J. Yang, X. Wang, J. Mater. Chem. A, 2019, 7, 21722-21729.
15 X. Teng, L. Guo, L. Ji, J. Wang, Y. Niu, Z. Hu, Z. Chen, ACS Appl. Energy Mater. 2019, 2, 5465-5471.
16 M. Gong, Y. Li, H. Wang, Y. Liang, J.Z. Wu, J. Zhou, J. Wang, T. Regier, F. Wei, H. Dai, J. Am. Chem. Soc. 2013, 135, 8452-8455.
17 Y. Wu, X. Tao, Y. Qing, H. Xu, F. Yang, S. Luo, C. Tian, M. Liu, X. Lu, Adv. Mater. 2019, 31, 1900178.
18 W.-D. Zhang, H. Yu, T. Li, Q.-T. Hu, Y. Gong, D.-Y. Zhang, Y. Liu, Q.-T. Fu, H.-Y. Zhu, X. Yan, Z.-G. Gu, Appl. Catal. B: Environ. 2020, 264, 118532.
19 Y. Tuo, X. Wang, C. Chen, X. Feng, Z. Liu, Y. Zhou, J. Zhang, Electrochim. Acta, 2020, 335, 135682.
20 R. Yang, Y. Zhou, Y. Xing, D. Li, D. Jiang, M. Chen, W. Shi, S. Yuan, Appl. Catal. B: Environ. 2019, 253, 131-139.
21 Y.X. Huang, X.J. Chen, S.P. Ge, Q.Q. Zhang, W.P. Li, Y.M. Cui, *Catal. Sci. Techn.*, **2020**, *10*, 1292-1298.
22 A. Kumar, S. Bhattacharyya, ACS Appl. Mater. Interfaces, 2017, 9, 41906-41915.
23 X.Z. Wen, *Int. J. Hydrogen Energy*, **2020**, *45*, 14660-14668.
24 Y. Liu, S. Jiang, S. Li, L. Zhou, Z. Li, J. Li, M. Shao, Appl. Catal. B: Environ. 2019, 247, 107-114.
25 D. Li, G. Hao, W. Guo, G. Liu, J. Li, Q. Zhao, J. Power Sources, 2019, 448, 227434.
26 M. Yao, H. Hu, B. Sun, N. Wang, W. Hu, S. Komarneni, Small, 2019, 15, 1905201.
27 Y. Wang, P. Zheng, M.X. Li, Y.R. Li, X. Zhang, J. Chen, X. Fang, Y.J. Liu, X.L. Yuan, X.P. Dai, H. Wang, *Nanoscale* **2020,** *12*, 9669-9679.
28 Y. Zhang, Q. Shao, Y. Pi, J. Guo, X. Huang, Small, 2017, 13, 1700355.
29 K. Huang, R. Dong, C. Wang, W. Li, H. Sun, B. Geng, *ACS Sustain. Chem. Eng.* **2019,** *7* (17), 15073-15079.
30 J. Tao, Y. Zhang, S. Wang, G. Wang, F. Hu, X. Yan, L. Hao, Z. Zuo, X. Yang, *ACS Appl. Mater. Interfaces* **2019,** *11* (20), 18342-18348.
31 M. Guo, S. Song, S. Zhang, Y. Yan, K. Zhan, J. Yang, B. Zhao, *ACS Sustain. Chem. Eng.* **2020,**

8 (19), 7436-7444.
32 X. Qiao, H. Kang, Y. Li, K. Cui, X. Jia, H. Liu, W. Qin, M. Pupucevski, G. Wu, *ACS Appl. Mater. Interfaces* **2020,** *12* (32), 36208-36219.
33 G. Rajeshkhanna, T. I. Singh, N. H. Kim, J. H. Lee, *ACS Appl. Mater. Interfaces* **2018,** *10* (49), 42453-42468.
34 K. Srinivas, Y. Lu, Y. Chen, W. Zhang, D. Yang, *ACS Sustain. Chem. Eng.* **2020,** *8* (9), 3820-3831.
35 X. Liu, Y. Yao, H. Zhang, L. Pan, C. Shi, X. Zhang, Z.F. Huang, J.J. Zou, *ACS Sustain. Chem. Eng.* **2020**, 8(48), 17828-17838.
36 G. B. Darband, M. Aliofkhazraei, S. Hyun, S. Shanmugam, *ACS Appl. Mater. Interfaces* **2020**, 12(48), 53719-53730.
37 D. Lim, E. Oh, C. Lim, S. E. Shim, S.H. Baeck, *Electrochi. Acta* **2020,** *361*, 137080.
38 Y. Wu, Y. Yi, Z. Sun, H. Sun, T. Guo, M. Zhang, L. Cui, K. Jiang, Y. Peng, J. Sun, *Chem. Eng. J.* **2020,** *390*, 124515.
39 H. Liao, X. Guo, Y. Hou, H. Liang, Z. Zhou, H. Yang, *Small* **2020,** *16* (10), e1905223.
40 M. Yao, H. Hu, B. Sun, N. Wang,W. Hu, S. Komarneni, *Small* **2019,** *15* (50), e1905201.
41 Y. K. Li, G. Zhang, W. T. Lu, F. F. Cao, *Adv. Sci.* **2020,** *7* (7), 1902034.